

MIT Open Access Articles

Integration of a Multiple-Condenser Loop Heat Pipe in a Compact Air-Cooled Heat Sink

The MIT Faculty has made this article openly available. *Please share* how this access benefits you. Your story matters.

Citation: Kariya, H. Arthur, Daniel F. Hanks, Wayne L. Staats, Nicholas A. Roche, Martin Cleary, Teresa B. Peters, John G. Brisson, and Evelyn N. Wang. "Integration of a Multiple-Condenser Loop Heat Pipe in a Compact Air-Cooled Heat Sink." Volume 2: Thermal Management; Data Centers and Energy Efficient Electronic Systems (July 16, 2013), Burlingame, CA, USA, ASME International, 2018. © 2018 ASME International

As Published: <http://dx.doi.org/10.1115/IPACK2013-73120>

Publisher: ASME International

Persistent URL: <http://hdl.handle.net/1721.1/119126>

Version: Final published version: final published article, as it appeared in a journal, conference proceedings, or other formally published context

Terms of Use: Article is made available in accordance with the publisher's policy and may be subject to US copyright law. Please refer to the publisher's site for terms of use.



IPACK2013-73120

INTEGRATION OF A MULTIPLE-CONDENSER LOOP HEAT PIPE IN A COMPACT AIR-COOLED HEAT SINK

H. Arthur Kariya, Daniel F. Hanks, Wayne L. Staats*, Nicholas A. Roche, Martin Cleary,
Teresa B. Peters, John G. Brisson and Evelyn N. Wang
Massachusetts Institute of Technology
Cambridge, MA, 02139, USA

*Currently at Sandia National Laboratory, Livermore, CA 94550.

ABSTRACT

We present the characterization of a compact, high performance air-cooled heat sink with an integrated loop heat pipe. In this configuration, heat enters the heat sink at the evaporator base and is transferred within the heat pipe by the latent heat of vaporization of a working fluid. From the condensers, the heat is transferred to the ambient air by an integrated fan. Multiple condensers are used to increase the surface area available for air-cooling, and to ensure the equal and optimal operation of the individual condensers, an additional wick is incorporated into the condensers. We demonstrated with this design (10.2 cm x 10.2 cm x 9 cm), a total thermal resistance of less than 0.1 °C/W while dissipating a heat load of 500 W from a source at 75 °C. Furthermore, constant thermal resistance was observed in the upright as well as sideways orientations. This prototype is a proof-of-concept demonstration of a high performance and efficient air-cooled heat sink design that can be readily integrated for various electronics packaging and data center applications.

INTRODUCTION

Loop heat pipes (LHPs) are passive two-phase devices that utilize the latent heat of vaporization to transfer heat, where vaporization and condensation occur in the evaporator and condenser, respectively. Due to the utilization of the latent heat of vaporization, LHPs have a high effective thermal conductivity between the evaporator and condenser, and are therefore promising solutions to thermal management of electronics [1, 2]. Since the working fluid is pumped in the LHP by capillary pressure, mechanical pumps are not required, resulting in significantly more compact and energy-efficient device. The practical application of LHPs in heat sinks,

however, must take into consideration the mechanism of heat transfer away from the LHP (air or liquid convection). The present study is a part of the development of novel heat sink that utilizes a 1) LHP with multiple planar condensers as a low thermal resistance, high surface area structure and 2) a fan impeller array interdigitated between the condensers for the reduction of the conductive and convective resistance in a compact form factor.

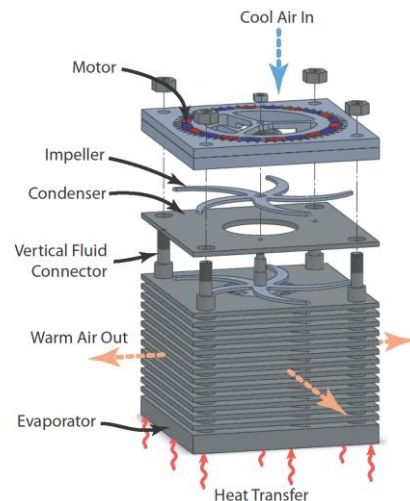


Figure 1. Schematic of air-cooled heat exchanger design. The layered structure constitutes the LHP. The thick bottom plate is the evaporator, and the multiple thin plates stacked above are the condensers. A low-profile motor is mounted on top of the structure, driving a shaft that spins the impeller blades that rotate between the condensers.

The developed heat sink is shown in Figure 1. Central to the design is the use of interdigitated multiple fan impellers and

the planar fins. A planar motor mounted to the top of the device drives the impeller array, drawing in cool ambient air from the top into the central core. The air then flows across the surface of the individual planar fins, cooling them, and is exhausted radially outwards. In this configuration, the use of the impeller to constantly sweep the air along the fin surface results in the enhancement of the convective heat transfer coefficient [3]. To reduce the conductive thermal resistance in the heat sink body, the entire structure is constructed from a LHP, where the heat input base is the evaporator, and the planar fins are multiple stacked condensers, which are connected by two vapor and two liquid lines at the corners. This heat sink configuration is expected to remove 1000 W with 10 condensers, for a thermal resistance of 0.05 °C/W (50 °C temperature difference between the evaporator base and the inlet air) [3].

This paper reports the characterization of a six-condenser version of the proposed design with emphasis on the operation of LHP; the dependence of the vapor temperature of the working fluid on the heat load and orientation are discussed.

LOOP HEAT PIPE DESIGN

Figure 2 shows a single-condenser schematic of the LHP and the circulation cycle of the working fluid, with cross sectional cuts made 1) in the condenser parallel to the condenser plane and 2) in the evaporator perpendicular to the condenser plane to show the internal features. Water is used as the working fluid due to its high surface tension, high latent heat of vaporization, and appropriate vapor-liquid (saturation) temperature range.

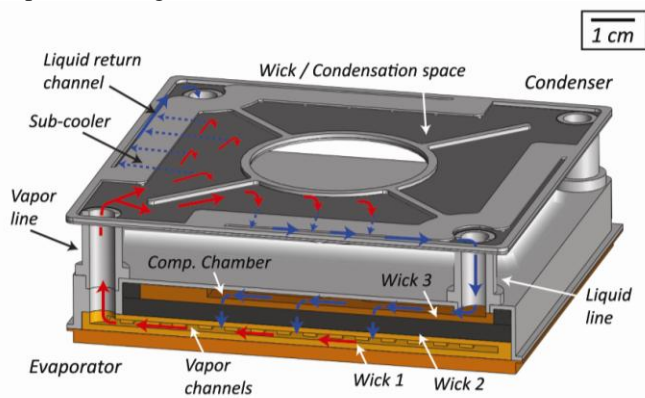


Figure 2. Cross-sectional schematic showing the internal features of the evaporator and condenser in a single-condenser LHP cycle. Sectional-cuts are made perpendicular to the plane of the evaporator and parallel to the plane of the condenser at mid-height to show the respective features. The arrows mark the circulation path of the working fluid, and the vapor and liquid phases are indicated by the red and blue arrows, respectively. The dashed arrows indicate flow through the wicks.

Application of heat to the evaporator results in vaporization at the surface of the vapor channels in the evaporator wick (1). The vapor flows through the network of vapor channels before exiting the evaporator, and enters the

condenser through a vertical vapor line. The vapor spreads across the open area of the condenser, which is lined with another wick (2). Air-cooling results in the condensation of the vapor onto the surface (menisci) of the condenser wick (3), after which the condensate flows radially outwards inside the wick, across a partition (“sub-cooler” in Figure 2), and into a liquid return channel to exit the condenser (4). The partition is used to separate the open vapor and liquid spaces in the condenser, and the wick is the only flow path between the two spaces. Continued cooling as the condensate flows across the partition ensures sufficient sub-cooling and prevents reevaporation (flashing). The condensate then flows down a vertical liquid line and into the top of the evaporator, which is called the “compensation chamber” (5) and is inherently at saturation (two-phase). The liquid is then drawn across the evaporator wick by capillary pressure back to the vapor channels, where the cycle repeats. A three-layer, monolithic wick structure is incorporated in the evaporator: 1) [Wick 1] for high thermal conductivity between the evaporator base and the vapor channels, 2) [Wick 2] for low thermal conductivity to establish a temperature gradient between the vapor channels and the compensation chamber, and 3) [Wick 3] for a high permeability, a low resistance path for the liquid to spread across the compensation chamber area when sections are blocked by the presence of vapor. Since saturation occurs in the vapor channels (at evaporation) as well as the compensation chamber, a temperature difference between these two locations results in a corresponding pressure difference. This pressure difference is critical for setting the direction of the circulation of the working fluid, as well as establishing capillary menisci (pressure) in the evaporator and condenser wicks.

The novel feature of this LHP design is the incorporation of a wick in the condenser, which is used to prevent the lower condensers from flooding with liquid. The stacked configuration of the condensers results in higher liquid pressures in the lower condensers due to the gravitational pressure head in the liquid line, despite relatively uniform vapor pressures. The higher liquid pressure can potentially cause the lower condensers to flood with liquid, substantially degrading their performance. By condensing onto the surface of a wick, menisci separate the vapor and liquid (condensate) phases and enable the generation of capillary pressure, which is used here to compensate for the different liquid pressures. The details of the design, fabrication and testing of the evaporator and condenser to enable this type of LHP operation are discussed in references [8 &9].

Figures 3 and 4 show fabricated samples of the condenser and evaporator, respectively. Both components were constructed through the high temperature processes of brazing, diffusion bonding and sintering to make the wicks from metal powder. Furthermore, for material compatibility with water, all components were fabricated from copper or Monel 400 (nickel-copper alloy, hereon “Monel”) [4-7]. Figure 3 shows half of a condenser, which was made by sintering a thin layer of Monel powder (0.5 mm thick) onto a chemically etched Monel frame (0.51-0.94 mm thickness). The condenser was designed

for a small volume (thickness) for a given surface area, and for a large internal area for condensation. Two halves were brazed together to complete a condenser. Figure 4 shows the three-layer wick structure in the evaporator; the copper-Monel wick was fabricated through a series of sintering steps where the sintering temperature was sequentially decreased to prevent over-sintering of the previously sintered layer(s). This procedure results in a monolithic wick 11.7 mm in thickness that is diffusion bonded to a Monel evaporator frame.

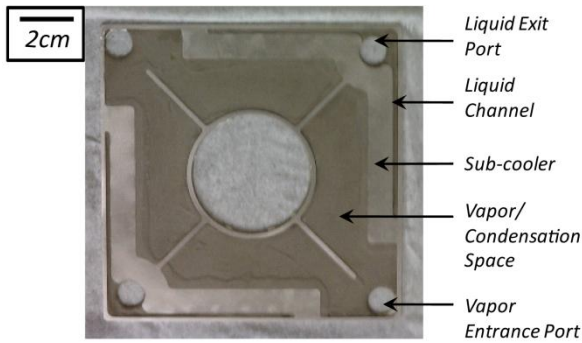


Figure 3. Photograph of a symmetric half of a condenser, showing the inner features. The wick is sintered inside of the condenser frame as a 0.5 mm layer, and lines not only the condensation space, but below the sub-cooler section as well. The outer surface of the condenser is smooth and planar. Two halves are brazed together to construct a full condenser, which has a footprint of 10 cm x 10 cm and a thickness of 2.5 mm.

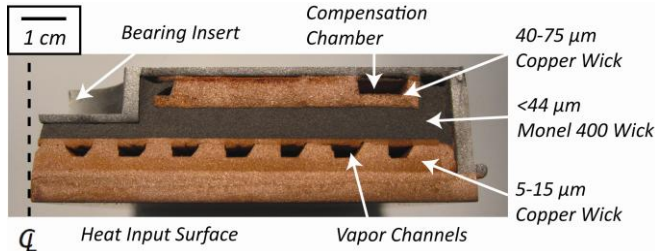


Figure 4. Cross-sectional photograph of a prototype evaporator, showing the three-layer wicking structure. The centerline of the evaporator is shown for reference; an insert is made in the evaporator frame for the impeller shaft bearing. The insulating wick (<44 μm, Monel 400) separates the vapor channels and compensation chamber, which are formed as channels within the high conductivity (5-15 μm, copper) and high permeability (40-75 μm, copper) wicks, respectively. The footprint and thickness of the evaporator are 10.2 cm x 10.2 cm and 1.6 cm, respectively.

TESTING OF THE SIX-CONDENSER LHP

The evaporator and condensers were fabricated separately and were assembled into a six-condenser, six-impeller heat sink (Figure 5A). The impeller shaft was positioned using two bearings at the ends; one bearing was inserted in the evaporator frame and the other was mounted in a bearing retaining plate near a custom-fabricated permanent synchronous magnet motor. The six-condenser format was constructed to demonstrate the proof-of-concept of a multiple-condenser LHP

that can operate without condenser flooding. The expected convective heat transfer coefficient in the air-flow between the condensers and the corresponding scaling of the convective thermal resistance with the number of condensers is described in references [3&10].

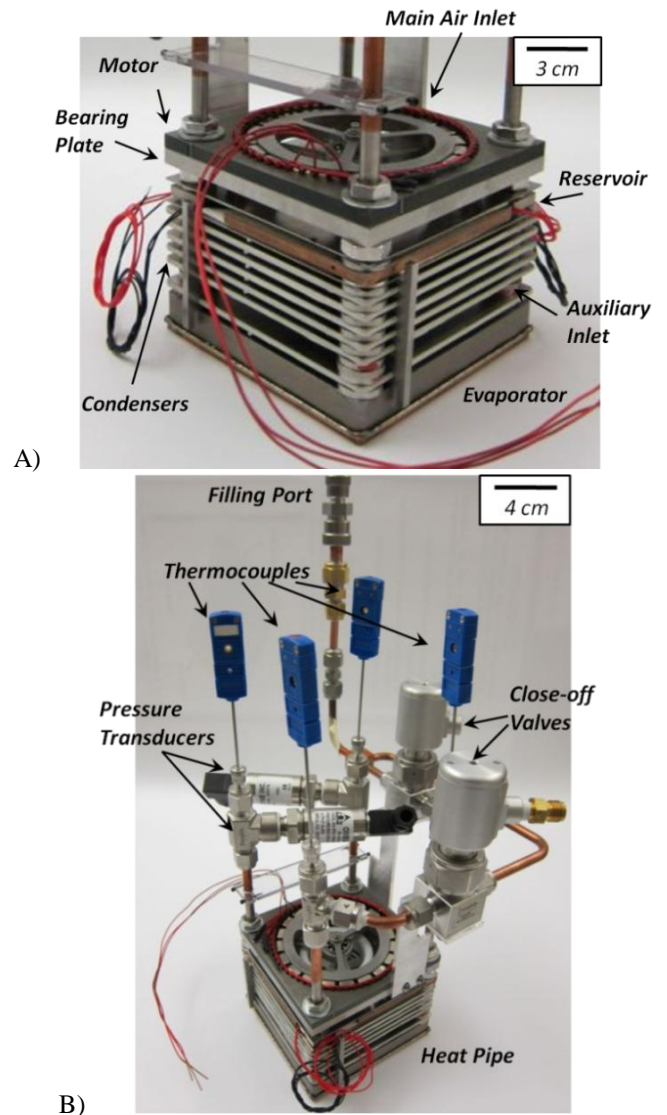


Figure 5. Experimental apparatus. A) Photograph of the six-condenser LHP and fan assembly. The six-condenser heat pipe consists of the evaporator, six, condensers, four tubes for liquid and vapor transport, and a reservoir. The reservoir allows for operation as a capillary pumped loop, and is not utilized in this study; the reservoir is therefore contains an additional, non-circulating volume of liquid. The fan assembly consists of a custom planar motor, six fan impellers, a central spindle shaft, two bearings and a bearing retaining plate. The shaft is located by the bearings in the bearing retaining plate and the evaporator. Air-flow into the apparatus occurs from the top (main inlet) as well as from the sides, near the evaporator (auxiliary inlet). B) Photograph of the LHP with a filling manifold and instrumentation. All sensors were installed above the LHP to avoid disturbing the LHP geometry.

The four vertical liquid and vapor lines extended beyond the height of the LHP; these lines were instrumented above the LHP to measure the temperatures and pressures of the liquid and vapor (Figure 5B). The temperatures of the individual condensers were measured by attaching thin-gauge thermocouple wires to the surface of the condensers in identical locations. Table 1 lists the sensors used and the corresponding accuracies.

Characterization was performed through two series of experiments. The thermal performance in the upright (evaporator at the bottom) orientation was tested at three fan speeds, 3500 RPM, 5000 RPM and 6000 RPM (± 50 RPM), by increasing the heat load. The effect of orientation was characterized by tilting the LHP after it reached steady state operation in the upright state at 150, 250 and 350 W at 5000 RPM. All tests were performed with the LHP filled to 91 mL, which was 4 mL less than the maximum liquid-side volume (95 mL), the volume that can be occupied by the liquid between the condenser and evaporator wicks. The 4 mL of under-filling compensated for the volumetric expansion of the liquid at elevated temperatures.

Table 1. Specifications of the sensors used in the experiment.

Measurement	Model	Accuracy
Vapor/Liquid Pressure	PX309-030A5V, Omegadyne	150 Pa
Vapor/Liquid Temperature	TMQSS-062U-10, Omega Eng.	0.4 °C
Evaporator Base Temp.	Nano Tube, Redfish	0.1 °C
Condenser Surface Temp.	5TC-TT-T-40-36, Omega Eng.	0.4 °C

RESULTS AND DISCUSSION

Thermal Performance in the Upright Orientation

Figure 6 shows the temperature response of the LHP, plotting the temperature difference between the vapor and ambient air against the applied heat load and fan speed. The ambient temperature varied between 22.3 and 24.5 °C, with a median of 23.4 °C. For heat loads above 150 W, the temperature difference increases linearly with heat load; the slope of this increase (average thermal resistance) was calculated using fit curves in this heat load range, and is also shown in Figure 6. In this linear regime, the primary thermal resistance of the device is that of the air-cooling, and consequently the thermal resistance can be decreased by increasing the fan speed, which results in a higher air flow rate and convective heat transfer coefficient. At a fan speed of 6000 RPM, a heat removal of 500 W was achieved at a thermal resistance of less than 0.1 °C/W. Higher heat loads were not tested due to the temperature limits of the pressure transducers.

The non-linearity below 150 W is attributed to the increased thermal resistance of the LHP through the flooding of the lower condensers. This effect can be seen in Figure 7, which plots the capillary pressure at the lowest condenser as a function of the heat load and fan speed. The capillary pressure

was absent for heat loads lower than 150 W, resulting in the flooding of the condenser.

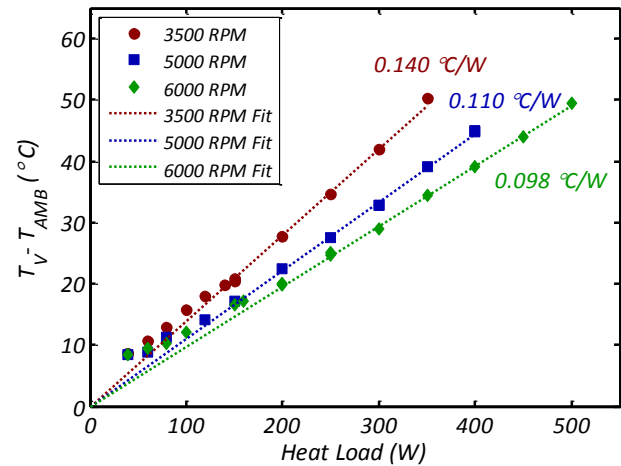


Figure 6. Temperature difference between the vapor and the ambient air, plotted against heat load and fan speed. The dotted lines show the linear fits for heat loads greater than 150 W, with a zero y-intercept, and were used to determine an average thermal resistance (slope). Heat loads higher than 150 W exhibit a linear temperature response, while lower heat loads result in a non-linear behavior due to condenser flooding. While an increase in heat load results in a higher temperature difference, higher fan speeds result in improved cooling and decrease the temperature difference.

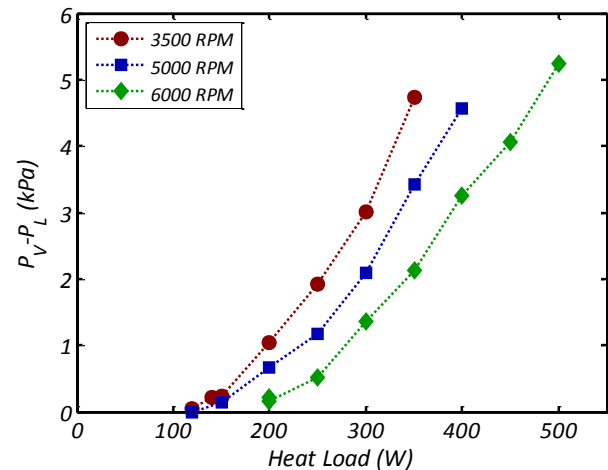


Figure 7. Capillary pressure, or the pressure difference between the vapor and liquid, in the lowest condenser. A positive capillary pressure indicates a receding meniscus; an advancing meniscus is assumed to hold negligible capillary pressure. The capillary pressure increases with heat load, and approaches zero at approximately 150 W; hence flooding is expected to occur below this critical heat load.

Effects of Orientation Change

The effect of orientation change was characterized by monitoring the temperatures as the LHP was tilted. In the discussion that follows, 0°, 90° and 135° of tilt refer to the upright, sideways and diagonally inverted orientations respectively. Figure 8 shows the temperature difference

between the vapor and the ambient air as a function of the tilt angle for three heat loads. While the figure shows the case of progressively increased tilt angles after startup from 0°, successful startup was observed for tilt angles up to 120°. For a given heat load the temperature difference is representative of the thermal resistance. The thermal resistance is relatively constant for tilt angles from 0° to 110° at 150 W and from 0° to 120° at 250 W and 350 W. The constant thermal resistance in this range of tilting is attributed to the presence of capillary pressure in the condensers, which maintains constant condensation behavior. At tilt angles beyond 120°, however, a substantial temperature increase was observed. As steady state operation was rarely achieved for these tilt angles, leading to heat pipe failure, the temperatures are not shown in Figure 8.

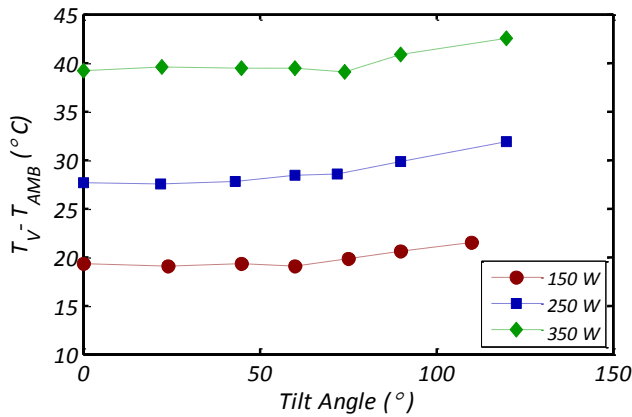


Figure 8. Temperature difference between the vapor and ambient air, plotted against the tilt angle and heat load at a fan speed of 5000 RPM. The temperature difference represents the thermal resistance for a given heat load, and is relatively constant with tilt angle up to 110° (150 W) and 120° (250W and 350W). Tilting the LHP to 135° resulted in either a substantial increase in vapor temperature or heat pipe failure, and the temperatures for this angle are not shown here due to the lack of repeatability.

Figure 9 shows the vapor and condenser surface temperatures plotted against the tilt angle. Condensers 1 and 6 refer to the condensers closest to and farthest from the evaporator, respectively. Note that due to the variability in the thermal attachment of the thermocouple onto the surface of the condensers, the condenser surface temperatures should not be compared with each other, and should only be used to assess the performance change of an individual condenser. For tilt angles less than 120°, the temperatures remain constant, signifying a constant thermal resistance. However, at 135°, the temperatures of the lower condensers decrease due to flooding, which results in excessive liquid in the condensers. As a result, the thermal resistance of the LHP increases, and a higher vapor temperature is required to remove the same amount of heat. Similarly, the upper, unflooded condenser needs to remove a comparatively greater amount of heat, and its temperature also rises. Although Figure 9 shows steady state temperatures for tilt angles from 0° to 120°, the temperatures at

135° were obtained 45 minutes into the experiment, during a steady temperature increase characteristic of heat pipe failure.

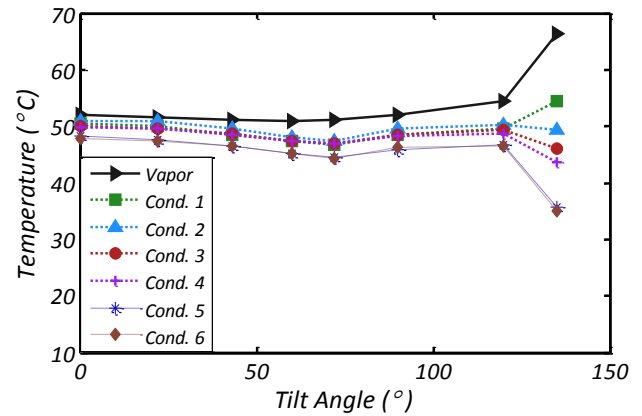


Figure 9. Vapor and condenser surface temperatures plotted as a function of the tilt angle, at 250 W and 5000 RPM. Condenser 1 indicates the condenser closest to the evaporator and 6 indicates that which is the farthest. As the condenser surface temperatures are measured by thin-gauge thermocouple wires taped onto the surface of the condensers, these measured temperatures should not be used to compare among condensers but to assess the performance change of a single condenser. The temperatures are constant for all tilt angles up to 120°. Flooding occurs at 135°, shown by the decrease in the temperatures of the lower condensers and the concomitant increase in vapor temperature.

CONCLUSION

We report the characterization of novel heat sink design which utilizes a multiple-condenser loop heat pipe (LHP) as the heat transfer surface. Use of multiple condensers enables the increase in heat transfer surface while maintaining a low conductive thermal resistance that is characteristic of LHPs. To ensure the equal operation of the condensers, a wick is integrated in the condensers to separate the vapor and liquid phases at condensation through a capillary meniscus. Operation with the lowest thermal resistance was achieved when capillary pressure was observed in the lowest condenser (> 150 W); a maximum heat removal of 500 W and a thermal resistance of 0.1 °C/W was achieved at a fan speed 6000 RPM. Furthermore, the LHP was operated through a range of orientations, with constant thermal resistance for all angles spanning the upright and sideways orientations. This work demonstrates the promise of using multiple condensers in LHPs for enhanced heat transfer and a new concept for high performance air-cooled heat exchangers.

ACKNOWLEDGMENTS

This work was supported by the Defense Advanced Research Projects Agency (DARPA) Microsystems Technology Office (MTO) Microtechnologies for Air-Cooled Exchangers (MACE) program, Grant Number W31P4Q-09-1-0007, with Dr. Thomas Kenny and Dr. Avram Bar-Cohen as the program managers.

REFERENCES

1. Maydanik Y.F., 2005. Review – Loop Heat Pipes, *Applied Thermal Engineering* 25(5-6): 635-657.
2. Ku J., 1999. Operating Characteristics of Loop Heat Pipes, SAE 1999-01-2007.
3. Staats, W.L. , 2012. *Active Heat Transfer Enhancement in Integrated Fan Heat Sinks*, Doctoral Thesis, Massachusetts Institute of Technology.
4. Rosenfeld, J.H. and N. Gernert, J., 2008. Life Test Results for Water Heat Pipes Operating at 200 °C to 300 °C, *Space Technology and Applications International Forum*.
5. Pittinato, G.F., 1978. Hydrogen Gas Generation in Water Heat Pipes. *Journal of Engineering Materials and Technology*, 100(3): 313-318.
6. Petrick, S.W., 1972. Hydrogen Gas Generation in Water/Stainless Steel Heat Pipes, *Winter Annual Meeting of the American Society of Mechanical Engineers*.
7. Anderson, W.G., et al., 2006. High Temperature Titanium/Water and Monel/Water Heat Pipes, *4th International Energy Conversion Engineering Conference and Exhibit*.
8. Hanks, D.F., 2012. *Design, Fabrication, and Characterization of a Multi-condenser Loop Heat Pipe*, Master's Thesis, Massachusetts Institute of Technology.
9. Kariya, H.A., 2012. *Development of an Air-cooled, Loop-type Heat Pipe with Multiple Condensers*, Doctoral Thesis, Massachusetts Institute of Technology.
10. Kariya, H.A., 2012. Scaling of the Performance of an Air-Cooled Heat Pipe with the Addition of Multiple Modular Condensers, *IEEE Intersociety Conference on Thermal and Thermomechanical Phenomena in Electronic Systems*